Copy No. 354

RM No. L9A18a

NACA

RESEARCH MEMORANDUM

INVESTIGATION AT A MACH NUMBER OF 1.9 AND A REYNOLDS NUMBER OF 2.2×10^6 OF SEVERAL FLAP-TYPE LATERAL-CONTROL DEVICES ON A WING HAVING 42.7° SWEEPBACK OF THE LEADING EDGE

By

Kennith L. Goin

Langley Aeronautical Laboratory
Langley Air Force Base, Va.

NATIONAL ADVISORY COMMITTEE
FOR AERONAUTICS
WASHINGTON
March 11, 1949

NATIONAL ADVISORY COMMITTEE FOR AERONAUTICS

RESEARCH MEMORANDUM

INVESTIGATION AT A MACH NUMBER OF 1.9 AND A REYNOLDS NUMBER OF 2.2×10^6 OF SEVERAL FLAP-TYPE LATERAL-CONTROL DEVICES ON A WING HAVING 42.7° SWEEPBACK OF THE LEADING EDGE

By Kennith L. Goin

SUMMARY

An investigation was made of various flap-type lateral-control devices on a wing having 42.7° sweepback of the leading edge at a Mach number of 1.90 and a Reynolds number of 2.2×10^6. Included were tests of several outboard ailerons, nose flaps, and a full-span aileron. The outboard ailerons tested consisted of a 20-percent-chord aileron with the basic (circular-arc) wing contour and several other ailerons having profiles which were obtained by (a) cusping, (b) flattening the sides, (c) flattening the sides and thickening the trailing edge, and (d) flattening the sides and extending the chord. The 15-percent-chord nose flaps tested had spans which were 40 percent and 60 percent that of the semispan model. The full-span aileron tested had the basic wing contour.

All the ailerons tested had positive rolling effectiveness which increased (for the outboard aileron) as the profile was changed by cusping, thickening the trailing edge, or extending the chord. The nose flaps tested were effective in roll. The rolling moments of the basic aileron and nose flaps were additive and independent. The 60-percent-span nose flap had a measured effectiveness in roll comparable with that of the outboard basic aileron. An increase of about 10 percent in minimum drag, over that of the wing with basic aileron, was measured for the extended-chord aileron and the aileron having trailing-edge thickness equal to hinge-line thickness. No appreciable effects of the other ailerons on drag were measured.

INTRODUCTION

Free-flight tests of a 42.7° sweptback wing equipped with 20-percent-chord flap-type outboard ailerons have indicated a reversal of aileron rolling effectiveness near a Mach number of 1 (reference 1). The reversal

was believed to be an effect of the large trailing-edge angle of the circular-arc-airfoil profile. An investigation of several aileron profiles, nose flaps, and full-span ailerons on the wing has been made at the Langley Aeronautical Laboratory in an effort to determine a satisfactory method of obtaining positive roll control. Included were free-flight tests at Mach numbers of 0.6 to 1.8 (references 1 and 2), transonic-bump tests at Mach numbers of 0.5 to 1.2 (references 3 and 4), and wind-tunnel tests at a Mach number of 1.90 (references 5 and 6).

Control-effectiveness test results (preliminary results reported in reference 5) obtained at a Mach number of 1.90 and a Reynolds number of 2.2×10^6 in the Langley 9- by 12-inch supersonic blowdown tunnel are summarized in this report. Included were tests of the basic (circular-arc) aileron and ailerons having profiles which were obtained by (a) cusping, (b) flattening the sides, (c) flattening the sides and thickening the trailing edge, and (d) flattening the sides and extending the chord. Tests of 15-percent-chord nose flaps having spans of 40 percent and 60 percent of the semispan model and test of a full-span basic aileron were also made.

SYMBOLS

C_L lift coefficient $\left(\frac{\text{Lift}}{qS}\right)$

C_D drag coefficient $\left(\frac{\text{Drag}}{qS}\right)$

C_m pitching-moment coefficient $\left(\frac{\text{Pitching moment about } 0.25\bar{c}}{qS\bar{c}}\right)$

C_l rolling-moment coefficient $\left(\frac{\text{Rolling moment about root chord}}{2qSb}\right)$

c local chord of airfoil in streamwise direction

b twice the distance from the wing root chord to the tip (12.000 in.)

$\bar{c}$ mean aerodynamic chord of entire wing (3.101 in.)

S entire area of semispan wing (17.943 sq in.)

q free-stream dynamic pressure

α angle of attack relative to free-stream direction

δ deflection of lateral-control device in a plane normal to the hinge line (positive for nose flap δ_n when leading edge is deflected upward and positive for aileron δ_a when trailing edge is deflected downward)

M Mach number

R Reynolds number based on $\bar{c}$

t ratio of trailing-edge thickness to thickness at 0.8c (aileron hinge line) for a series of flat-side ailerons

MODELS AND TESTS

The semispan-wing model was tested alone and in the presence of a half fuselage (fig. 1). The principal dimensions are shown in figure 2 for the fuselage-off configuration and in figure 3 for the fuselage-on configuration. The wing had a leading-edge sweepback of 42.7°, an aspect ratio of 4, a taper ratio of 0.5, and an airfoil section normal to the quarter-chord line which very closely approximated a 10-percent-thick circular-arc section. The sections in the streamwise direction were approximately 8 percent thick with ordinates as given in table I.

Two steel wings (identical within construction tolerances) and a brass fuselage, all having polished surfaces, were used for these tests. The two wings were necessary to cover the desired range of test configurations.

The outboard ailerons tested are shown in figure 2. The contour of the basic aileron was made to conform to the wing profile. The cusped, $t = 0.0$, $t = 0.5$, and $t = 1.0$ ailerons had the same plan form as the basic aileron. The extended-chord aileron had flat sides and a chord twice that of the basic aileron. The full-span aileron, as shown in figure 3, had the same contour as the basic aileron and extended from 0.13 to $0.96\frac{b}{2}$. The hinge line for all ailerons tested was located at approximately 0.80c. The contours of the nose flaps extending from 0.6 to $1.0\frac{b}{2}$ and from 0.4 to $1.0\frac{b}{2}$ were formed by the basic wing contour. The hinge line was located at 0.15c and in a plane near one surface of the wing. The installations of the ailerons and nose flaps simulated sealed unbalanced flap-type control devices. Details of the installations and directions of deflections are shown in figure 2.

TUNNEL AND TEST TECHNIQUE

The present tests were made in the Langley 9- by 12-inch supersonic blowdown tunnel at a Mach number of 1.90. This tunnel is a nonreturn-type tunnel which utilizes the exhaust air of the 19-foot pressure tunnel.

The dynamic pressure and Reynolds number decreased about 5 percent during each run because of decreasing pressure of the inlet air.

Two methods were used in mounting the wing alone in the tunnel. The data for wing 1 (table II) were obtained from tests with the model attached to a 4-inch-diameter disk the face of which was flush with the tunnel floor. The remaining data are from tests with wing 2 mounted through a similar disk which was not attached to the model or balance but which rotated through the angle-of-attack range with the model. Tests of the basic aileron on wings 1 and 2 show no measurable differences resulting from the two methods of mounting or the two models used.

During tests with the wing in the presence of a half-fuselage, only forces on the wing were measured. The installation for this configuration is described in reference 6.

The semispan-wing model was in all cases cantilevered from a four-component strain-gage balance which was attached to the tunnel floor. The balance rotated through the angle-of-attack range with the model and measured normal force, chord force, pitching moment, and rolling moment due to normal force.

The inboard end of the wing was used as a reference axis for rolling moments in all cases even though it was displaced from the fuselage center line during fuselage-on tests (fig. 3) in order to give an exposed wing area comparable with that of references 3 and 4.

PRECISION OF DATA

Free-stream Mach number has been calibrated at 1.90 ± 0.02. This Mach number was used in determining the dynamic pressure on which all the present data are based. Various factors which might possibly affect the test results of this tunnel are discussed in reference 7. Condensation of moisture is one of these (the inlet air which enters at a pressure of $2\frac{1}{3}$ atmospheres contains about 0.003 pound of water per pound of air). With regard to the wing-alone test arrangement, not considered in reference 7, the effects of the 0.4-inch-thick tunnel-wall boundary layer are not known. It is believed, however, that no large errors are present because the theoretical wing-alone lift-curve slope of 0.045 is in reasonable agreement with the experimental value of 0.041. In any event the outboard aileron and nose-flap characteristics should show little, if any, effects of the wing-root boundary layer.

The accuracy of measurements for low aileron deflections is believed to be of the order indicated in the following table:

Variable:	Error
α	±0.05°
δ_a	.2°
δ_n	.2°
C_L	.005
C_l	.0003
C_m	.001
C_D	.001

For aileron deflections of about 15° C_l, C_m, and C_D showed unsteadiness which resulted in errors somewhat greater than those indicated in the table.

RESULTS AND DISCUSSION

The test results for the basic aileron without fuselage are presented in figure 4 showing the variation of each aerodynamic coefficient with angle of attack for the various control-surface deflections. Except for drag, the curves for each of the coefficients were linear and parallel within the investigated range of angle of attack and control-surface deflection. Such families of linear parallel curves were found to occur for each of the remaining configurations. Accordingly, the test data have not been presented, but cross plots are given which show only the increment relative to zero deflection, of each aerodynamic coefficient plotted against control-surface deflection (figs. 5 to 10). For the drag cross plots the actual faired values, rather than the increments, are plotted for zero angle of attack. Because of the frequent close grouping of the cross-plot points, symbols have been used in the cross plots (figs. 5 to 10) to aid in identifying the various configurations. Some of the more important aerodynamic characteristics have been summarized in table II. The rolling-effectiveness data (figs. 5 and 6 and table II) are applicable to a complete wing with deflections of one aileron or nose flap. Lift, drag, and pitching-moment characteristics (figs. 7 to 10 and table II) apply to a semispan wing with positive deflections of the aileron or nose flap.

The data pertaining to the cusped, extended-chord, and basic aileron have been published previously in reference 5. It has been found since the presentation of these data, however, that deflection of the strain-gage balance, resulting from model pitching moments, made necessary a correction to angle of attack. The small differences existing between the data presented herein and those of reference 5 are a result of these angle-of-attack corrections which have been applied to all the present data.

The data presented include several repeat tests of the partial-span basic and $t = 0.5$ ailerons. In view of the amount and consistency of test data, it is believed that values of $\frac{dC_l}{d\delta_a}$ for these two ailerons, as presented in table II, are accurate to about ±6 percent. For the other ailerons and nose flaps where only one set of data is available the accuracy is believed to be about ±10 percent.

ROLLING MOMENTS

Ailerons.- The rolling effectiveness $\frac{dC_l}{d\delta_a}$ of the six outboard ailerons and the full-span aileron is shown in figure 5 and table II. The effectiveness of the $t = 0.0$ aileron was the same as that for the basic aileron. An increase in effectiveness, over that of the basic aileron, of about 10 percent for the cusped and $t = 0.5$ ailerons, 50 percent for the $t = 1.0$ aileron, 100 percent for the extended-chord aileron, and 30 percent for the full-span basic aileron (when tested in the presence of a fuselage) was shown. No appreciable effects of the fuselage on outboard aileron characteristics were measured. Changing the aileron profile from basic to $t = 0.5$ caused an increase of about 40 percent in hinge moments at a Mach number of 1.90 as compared with the increase of about 10 percent in rolling effectiveness. (See reference 6.)

With regard to the usefulness of these ailerons, transonic-bump tests indicated that the reversal in aileron effectiveness in the transonic speed range would not be materially improved by cusping or flattening the sides $(t = 0.0)$ of the basic aileron (reference 3). Positive effectiveness was obtained in bump and free-flight tests, however, by extending the aileron chord to at least 0.32c or by thickening the aileron trailing edge to at least $t = 0.5$ (references 2, 3, and 4).

Nose flaps.- Both the nose flaps tested were effective in producing roll, but no effect of either on aileron rolling-moment characteristics was shown (fig. 6). The value of $\frac{dC_l}{d\delta}$ was 0.00022 for the $0.4\frac{b}{2}$ nose flap and 0.00035 for the $0.6\frac{b}{2}$ nose flap compared with 0.00034 for the basic aileron. Calculated hinge moments for the $0.6\frac{b}{2}$ nose flap (for which the second-order method of reference 6 should be fairly accurate) were of the order of twice those for the basic aileron. That is, for the same deflection (and practically the same experimental rolling effectiveness), the nose flap had twice as much hinge moment as did the aileron. This greater magnitude in hinge moment does not

appear unreasonable if it is remembered that deflecting the nose flap not only causes a change in loading on the flap but also causes a change in loading of the opposite sign on the portion of the wing behind the nose flap. Data presented in reference 3 indicate that in the transonic speed range the $0.4\frac{b}{2}$ nose flap is ineffective as a control device and has an adverse effect on aileron roll characteristics.

LIFT, DRAG, AND PITCHING MOMENT

Ailerons.- The lift, drag, and pitching-moment characteristics of the wing with the various ailerons tested are shown in figures 7 and 8 and are summarized in table II. These characteristics of the wing with cusped, $t = 0.0$ and $t = 0.5$ ailerons were essentially the same as those with the basic aileron. Values of $\frac{dC_L}{d\delta_a}$ and $\frac{-dC_m}{d\delta_a}$ were increased by the $t = 1.0$ aileron and were increased further by the extended-chord aileron. A trend was noted toward increasing wing lift-curve slope and rearward shift of chordwise center of pressure as the aileron trailing edge was thickened or as the aileron chord was extended (table II). Although the trend toward increasing lift-curve slope was within the estimated accuracy of the data for the $t = 0.0$ and $t = 0.5$ ailerons, substantial increments were measured for the $t = 1.0$ and extended-chord ailerons. As a matter of interest, increasing the span of the outboard basic aileron to full span caused an increase in $\frac{dC_L}{d\delta_a}$ approximately in proportion to the increase in area. No appreciable effects of aileron profile on drag were measured except for the $t = 1.0$ and extended-chord ailerons where an increase of about 10 percent in $C_{D_{min}}$ (corresponding to an increase of about 25 percent in section drag) over that for the basic aileron was shown. Reference 4 indicates an increase in drag for the $t = 0.5$ aileron, however, and a considerably larger increase for the $t = 1.0$ aileron in the high subsonic and transonic speed range.

Nose flaps.- The ratio of $\frac{dC_L}{d\delta}$ to control-surface area was about 25 percent higher for the nose flaps than for the basic aileron. The increments of lift contributed by the basic aileron and nose flaps were additive and independent. There were no effects of the nose flaps on C_m with the nose flaps deflected either alone or in combination with the basic aileron (figs. 9 and 10) although the greater portions of the nose-flap lifting surface were behind the pitching-moment reference axis. The negative pitching moment expected because of the increased upload on

the flap apparently was canceled by a positive pitching moment resulting from an induced download on the wing panel behind the flap. The download, though of smaller magnitude than the upload, would be operating at a considerably greater distance behind the pitch axis than the flap. The increase in wing drag caused by the deflection of either nose flap was somewhat greater than that caused by basic aileron deflection.

CONCLUSIONS

From tests of a wing having 42.7° sweepback of the leading edge and having biconvex sections, the following conclusions may be drawn concerning characteristics at a Mach number of 1.90:

1. All the ailerons tested had positive rolling effectiveness. An increased effectiveness was shown as the aileron profile was changed from that of the basic (circular-arc) aileron by cusping, extending the chord, or thickening the trailing edge.

2. The 15-percent-chord nose flaps tested were effective in producing roll. The 60-percent-semispan nose flap had approximately the same rolling effectiveness as the basic aileron.

3. The rolling moments contributed by the basic aileron and nose flaps were additive and independent.

4. No appreciable effects of aileron profile on drag were measured except for the extended-chord aileron and the aileron having trailing-edge thickness equal to the hinge-line thickness. An increase of about 10 percent in minimum drag was measured with these ailerons.

Langley Aeronautical Laboratory
National Advisory Committee for Aeronautics
Langley Air Force Base, Va.

REFERENCES

1. Sandahl, Carl A.: Free-Flight Investigation at Transonic and Supersonic Speeds of the Rolling Effectiveness of a 42.7° Sweptback Wing Having Partial-Span Ailerons. NACA RM No. L8E25, 1948.

2. Sandahl, Carl A.: Free-Flight Investigation at Transonic and Supersonic Speeds of the Rolling Effectiveness of Several Aileron Configurations on a Tapered Wing Having 42.7° Sweepback. NACA RM No. L8K23, 1948.

3. Turner, Thomas R., Lockwood, Vernard E., and Vogler, Raymond D.: Preliminary Investigation of Various Ailerons on a 42° Sweptback Wing for Lateral Control at Transonic Speeds. NACA RM No. L8D21, 1948.

4. Turner, Thomas R., Lockwood, Vernard E., and Vogler, Raymond D.: Aerodynamic Characteristics at Subsonic and Transonic Speeds of a 42.7° Sweptback Wing Model Having an Aileron with Finite Trailing-Edge Thickness. NACA RM No. L8K02, 1948.

5. Sivells, James C., and Conner, D. William: Preliminary Investigation at a Mach Number of 1.9 and a Reynolds Number of 2,200,000 of Three Ailerons Applicable to the Bell XS-2 Airplane Design. NACA RM No. L8D02, 1948.

6. Sivells, James C., and Goin, Kennith L.: Experimental and Calculated Hinge Moments of Two Ailerons on a 42.7° Sweptback Wing at a Mach Number of 1.9. NACA RM No. L8K24a, 1949.

7. Conner, D. William: Aerodynamic Characteristics of Two All-Movable Wings Tested in the Presence of a Fuselage at a Mach Number of 1.9. NACA RM No. L8H04, 1948.

TABLE I

ORDINATES FOR AIRFOIL SECTION OF 42.7°

SWEPTBACK TAPERED WING

[Stations and ordinates given in percent airfoil chord in free-stream direction; section symmetrical about chord line]

Station	Ordinate
0	0
5	.712
10	1.357
15	1.935
20	2.444
25	2.884
30	3.253
35	3.549
40	3.772
45	3.919
50	3.989
55	3.981
60	3.892
65	3.720
70	3.463
75	3.120
80	2.686
85	2.161
90	1.540
95	.821
100	0

NACA

TABLE II

CHARACTERISTICS OF A 42.7° SWEPTBACK WING WITH SEVERAL

TYPES OF AILERONS AND NOSE FLAPS

Wing	Control device	Description	Fuselage	$\frac{dC_l}{d\delta}$	$\frac{dC_L}{d\delta}$	$\frac{dC_m}{d\delta}$	$C_{D_{min}}$	$\frac{dC_L}{d\alpha}$	$\frac{dC_m}{dC_L}$
1 and 2	Aileron	Basic	Off	0.00034	0.0018	-0.0019	0.030	0.041	-0.18
1		Cusped		.00037	.0019	.0019	.031	.041	.18
1		Extended chord		.00070	.0044	.0044	.033	.044	.23
2		t = 0.0		.00034	.0017	.0018	.031	.041	.18
2		t = 0.5		.00038	.0020	.0018	.030	.041	.19
1		t = 1.0		.00050	.0028	.0027	.034	.042	.20
2		Full span basic	On	.00043	.0038	.0026	.025	.037	.25
2		Outboard basic		.00034	.0017	.0017	.025	.037	.25
1	0.15c Nose flap	$0.4\frac{b}{2}$	Off	.00022	.0014	.0000	.030	.041	.18
1		$0.6\frac{b}{2}$		.00035	.0022	.0000	.030	.041	.18

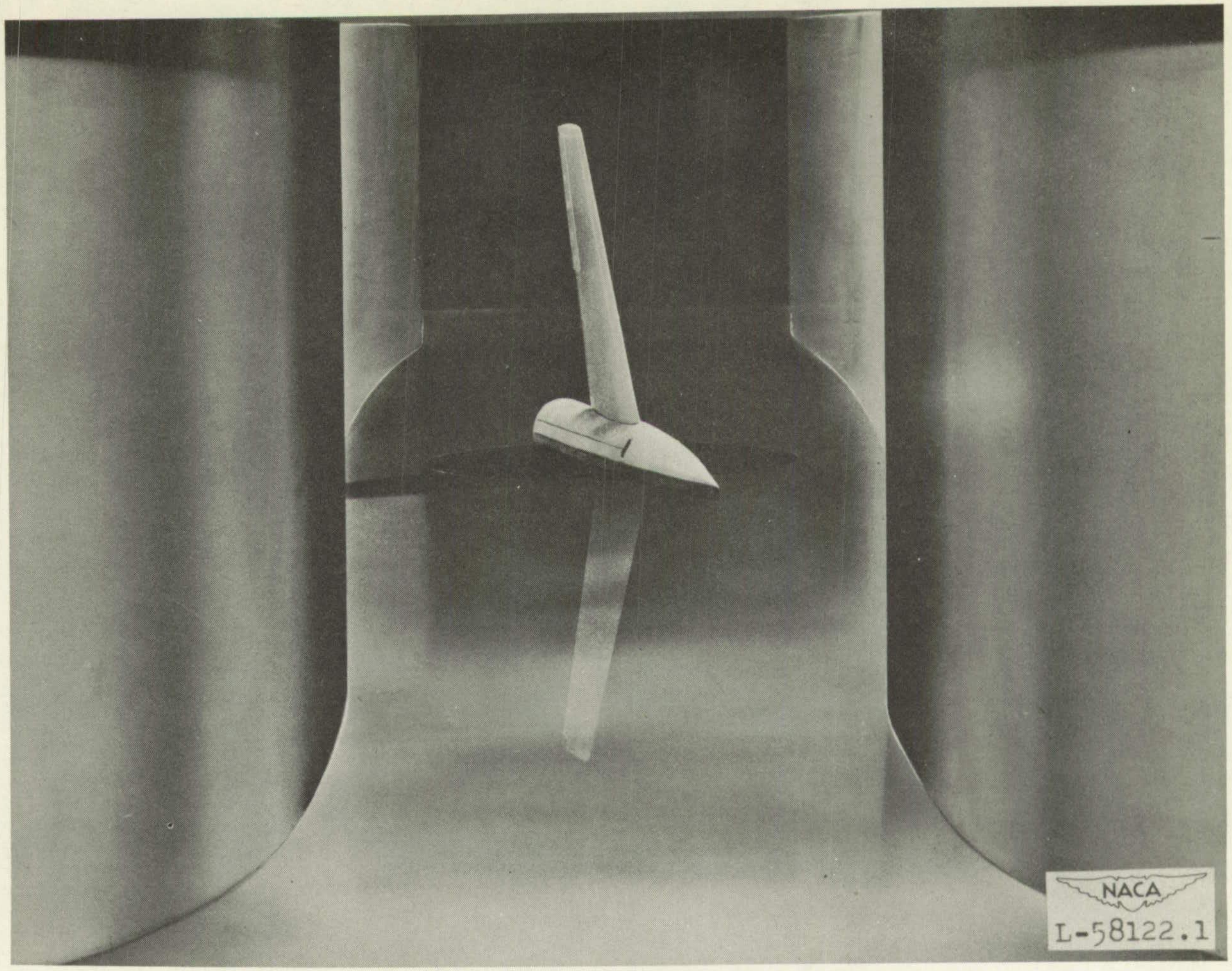

(a) Model mounted in test section of the Langley 9- by 12-inch supersonic blowdown tunnel.

Figure 1.- 42.7° semispan-wing model and fuselage.

CONFIDENTIAL

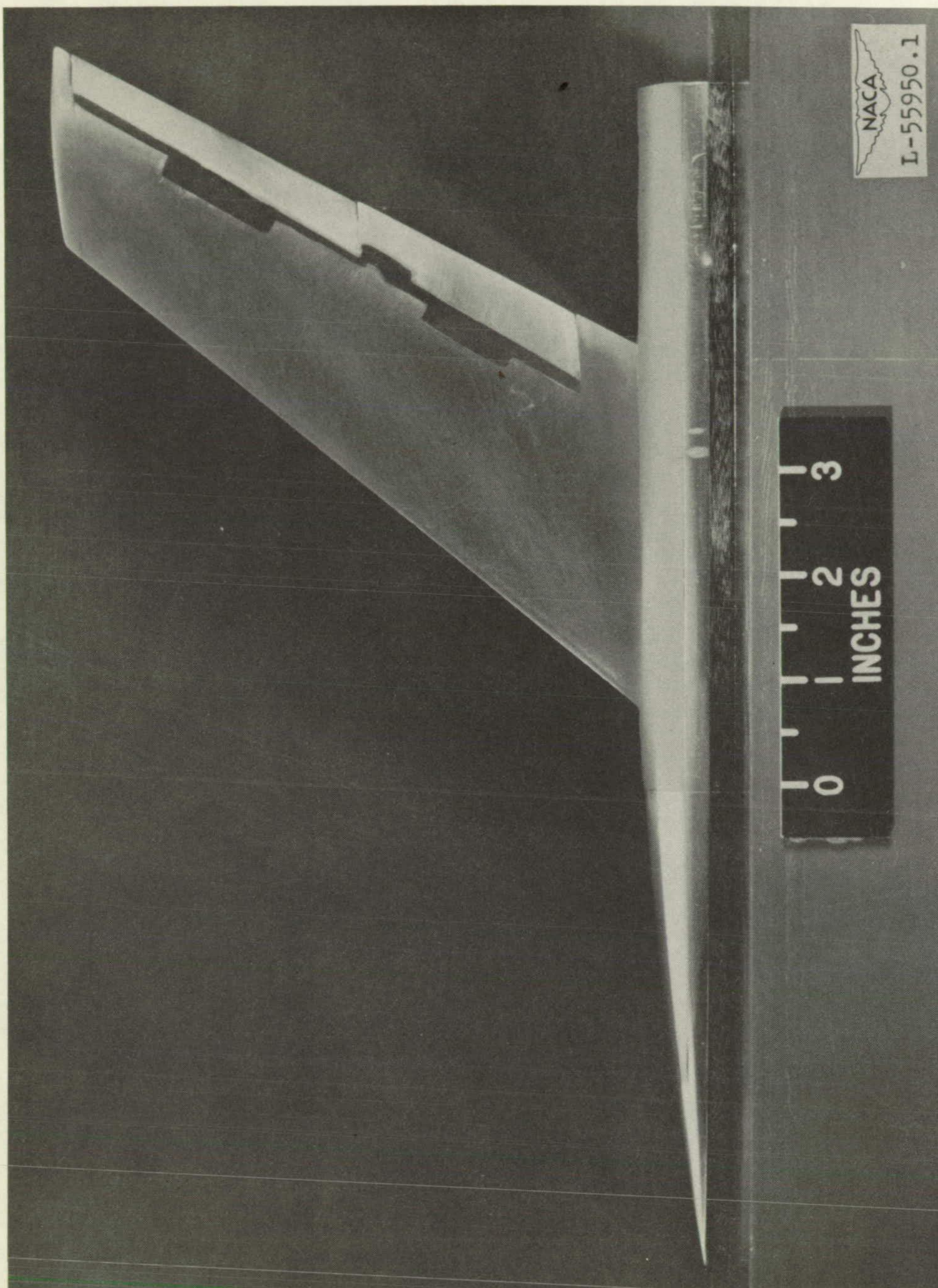

(b) Close-up of wing and fuselage.

Figure 1.- Concluded.

CONFIDENTIAL

CONFIDENTIAL

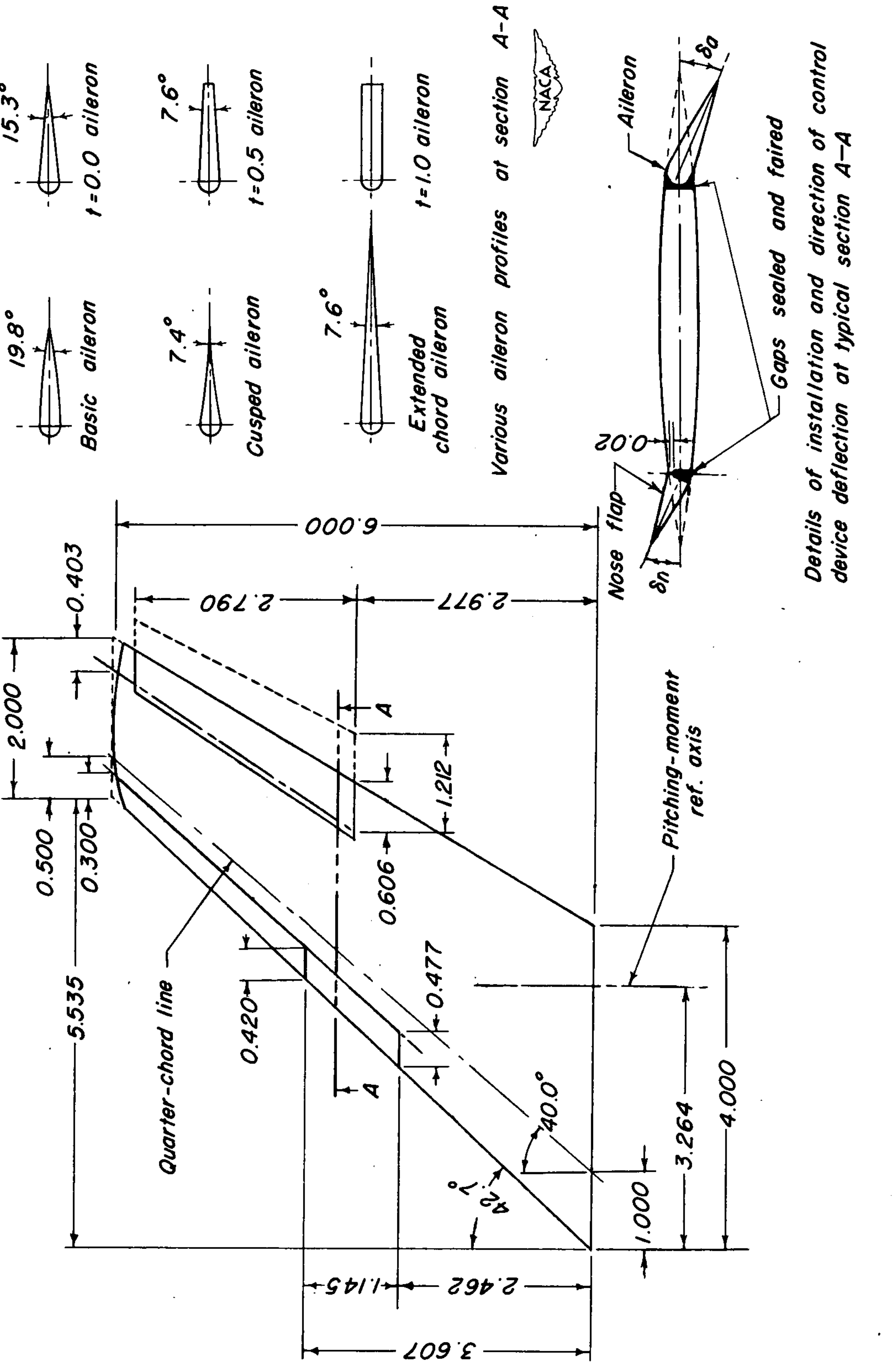

Figure 2.— Details of 42.7° sweptback wing, ailerons and nose flaps. (All dimensions in inches.)

CONFIDENTIAL

CONFIDENTIAL

Fuselage ordinates	
Station	Radius
0	0
0.676	0.117
1.353	.225
2.029	.325
2.706	.413
3.382	.489
4.059	.555
4.735	.613
5.412	.649
6.088	.672
6.765	.676
12.250	.676

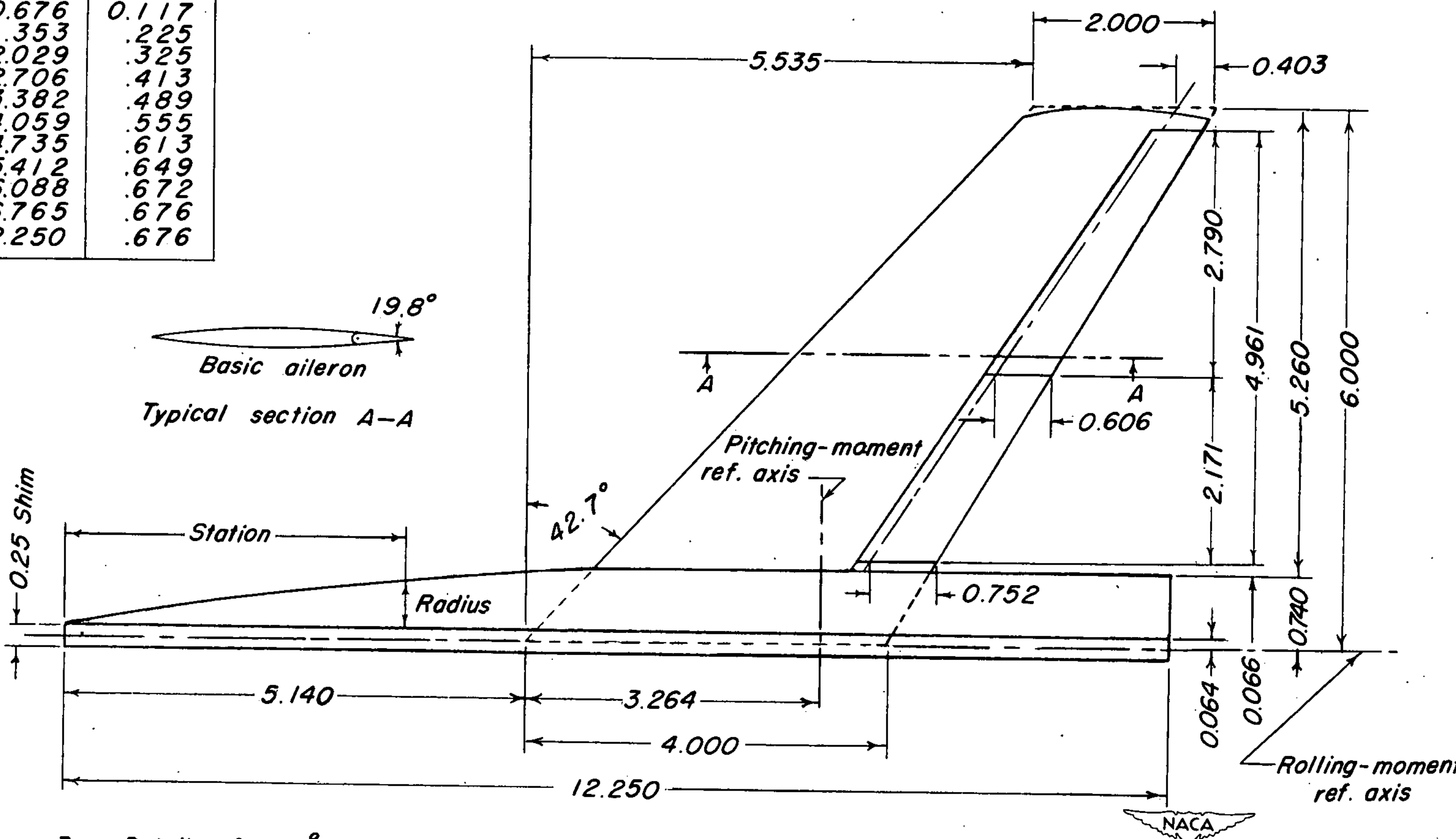

Figure 3.— Details of 42.7° sweptback wing, outboard and full span ailerons, and fuselage. Area outboard aileron, 1.430 sq in.; area full-span aileron, 2.905 sq in.; area wing, 17.943 sq in.; $\bar{c}$, 3.101 in. (All dimensions in inches.)

CONFIDENTIAL

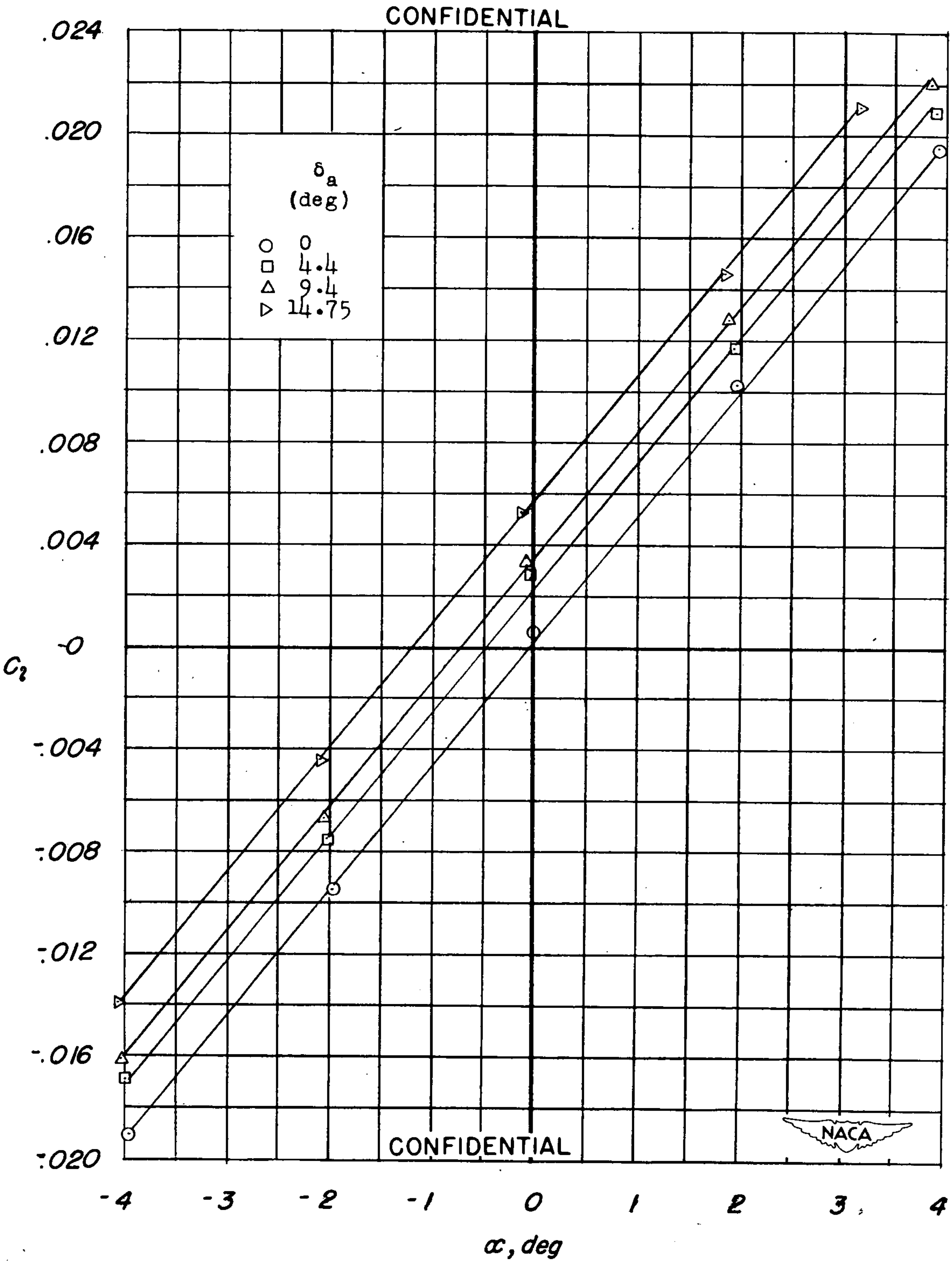

(a) C_l plotted against α.

Figure 4.- Aerodynamic characteristics of a 42.7° sweptback wing with basic aileron. Fuselage off; M = 1.9 ; R = 2.2 x 10^6.

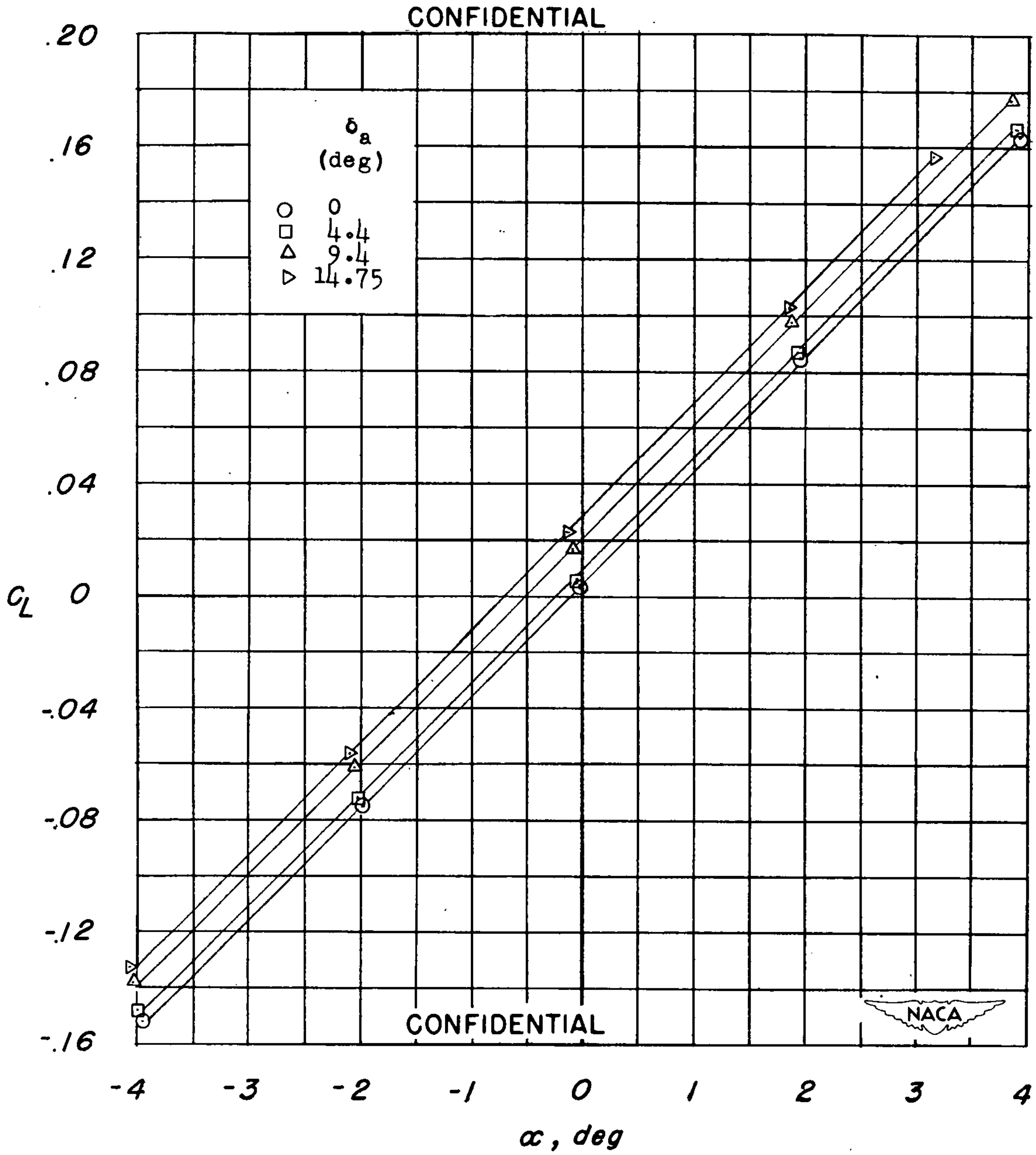

(b) C_L plotted against α.

Figure 4.- Continued.

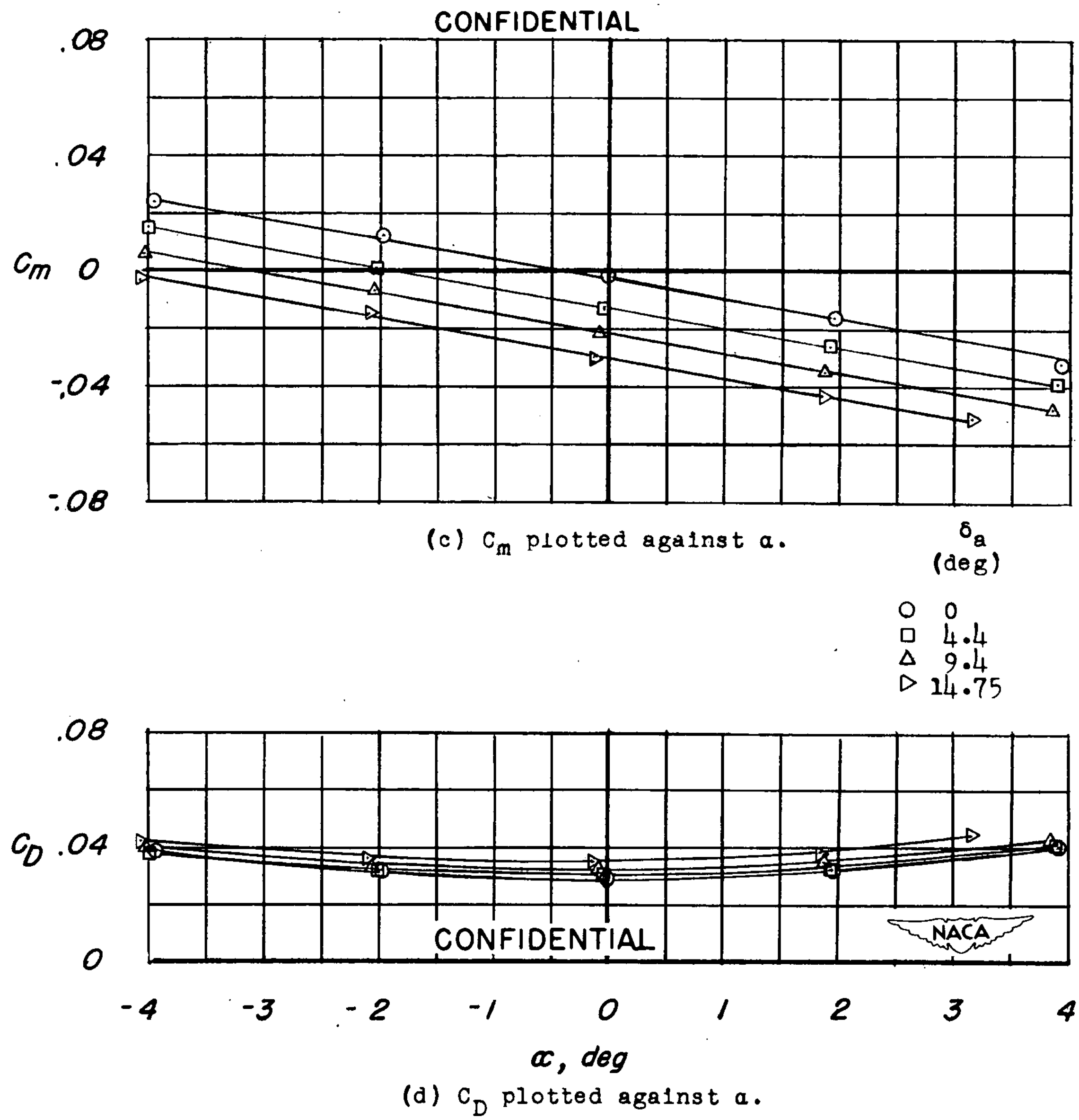

Figure 4.- Concluded.

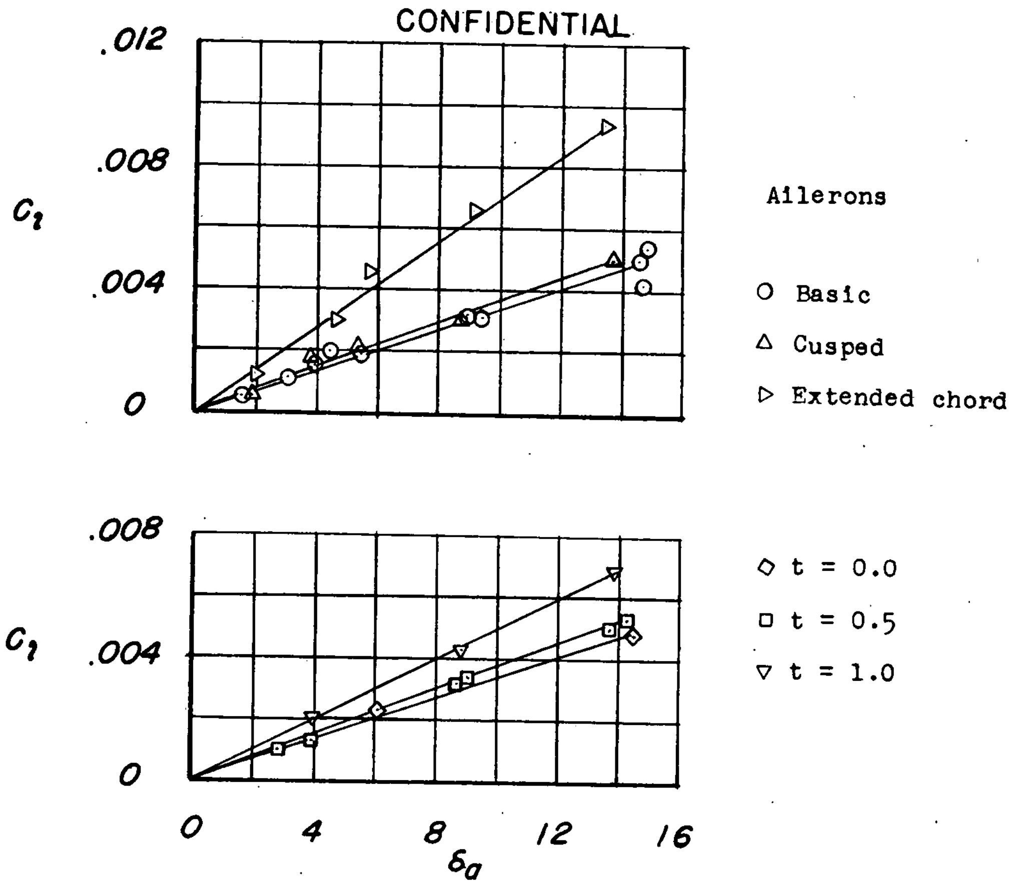

(a) Effect of aileron profile, fuselage off.

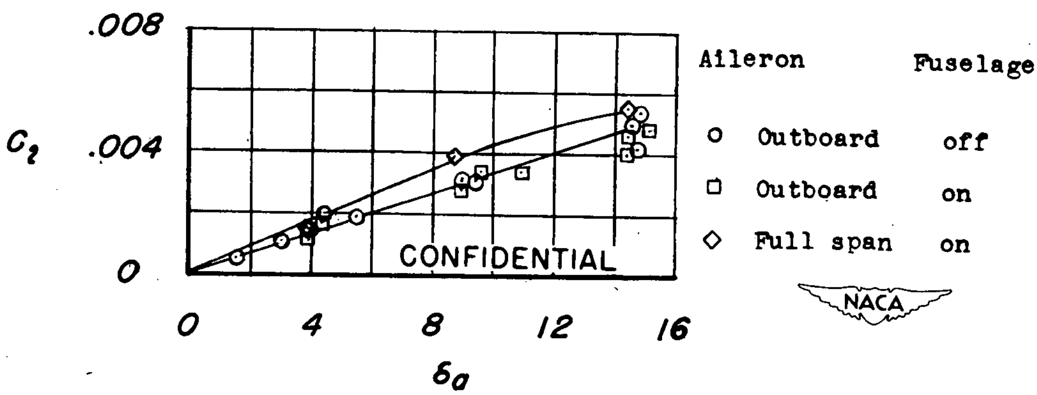

(b) Effect of aileron span.

Figure 5.- Comparison of rolling-moment characteristics of several aileron configurations on a 42.7° sweptback wing. $\alpha = 0^\circ$ to 4°; $M = 1.9$; $R = 2.2 \times 10^6$. Symbols designate cross-plot points taken from faired curves.

CONFIDENTIAL

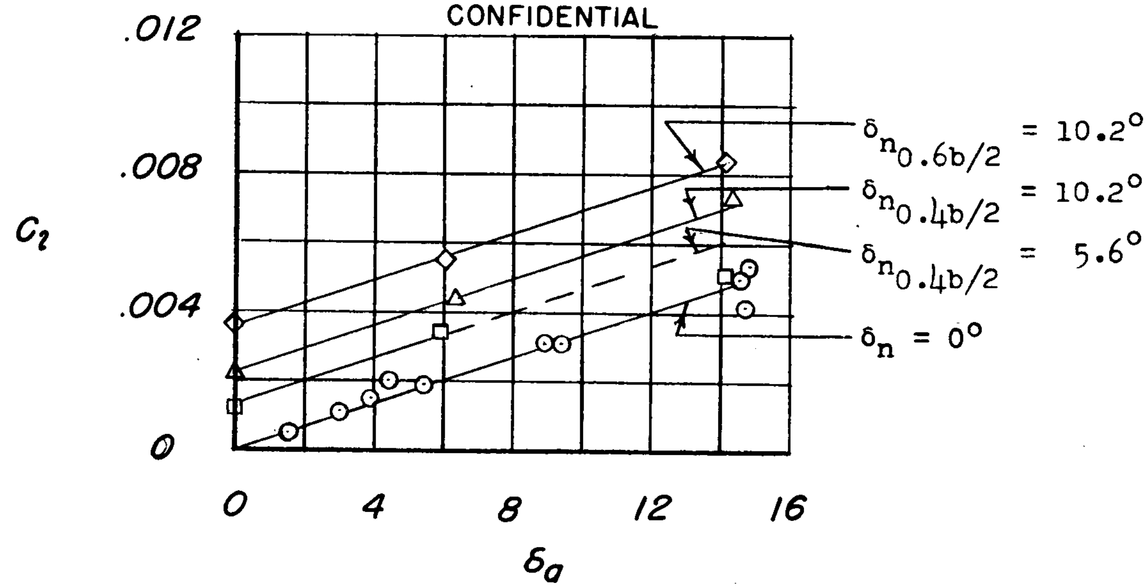

(a) Effectiveness of basic aileron with nose flaps deflected.

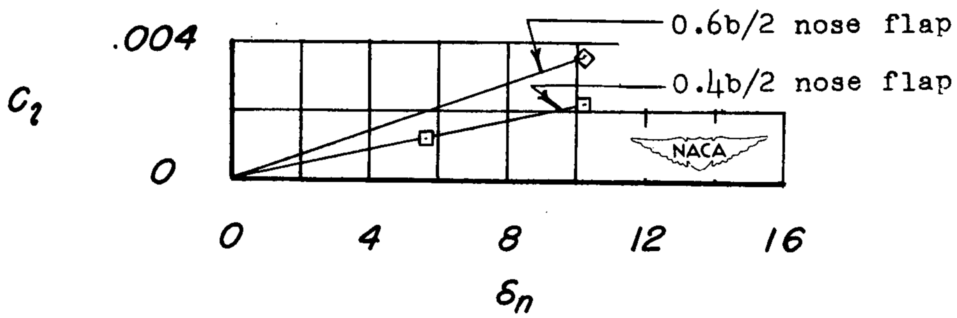

(b) Effectiveness of nose flaps. $\delta_a = 0^\circ$.

Figure 6.- Rolling-moment characteristics of 0.15c nose flaps on 42.7° sweptback wing. Fuselage off; $\alpha = 0^\circ$ to 4°; M = 1.9; R = 2.2 x 10^6. Symbols designate cross-plot points taken from faired curves.

CONFIDENTIAL

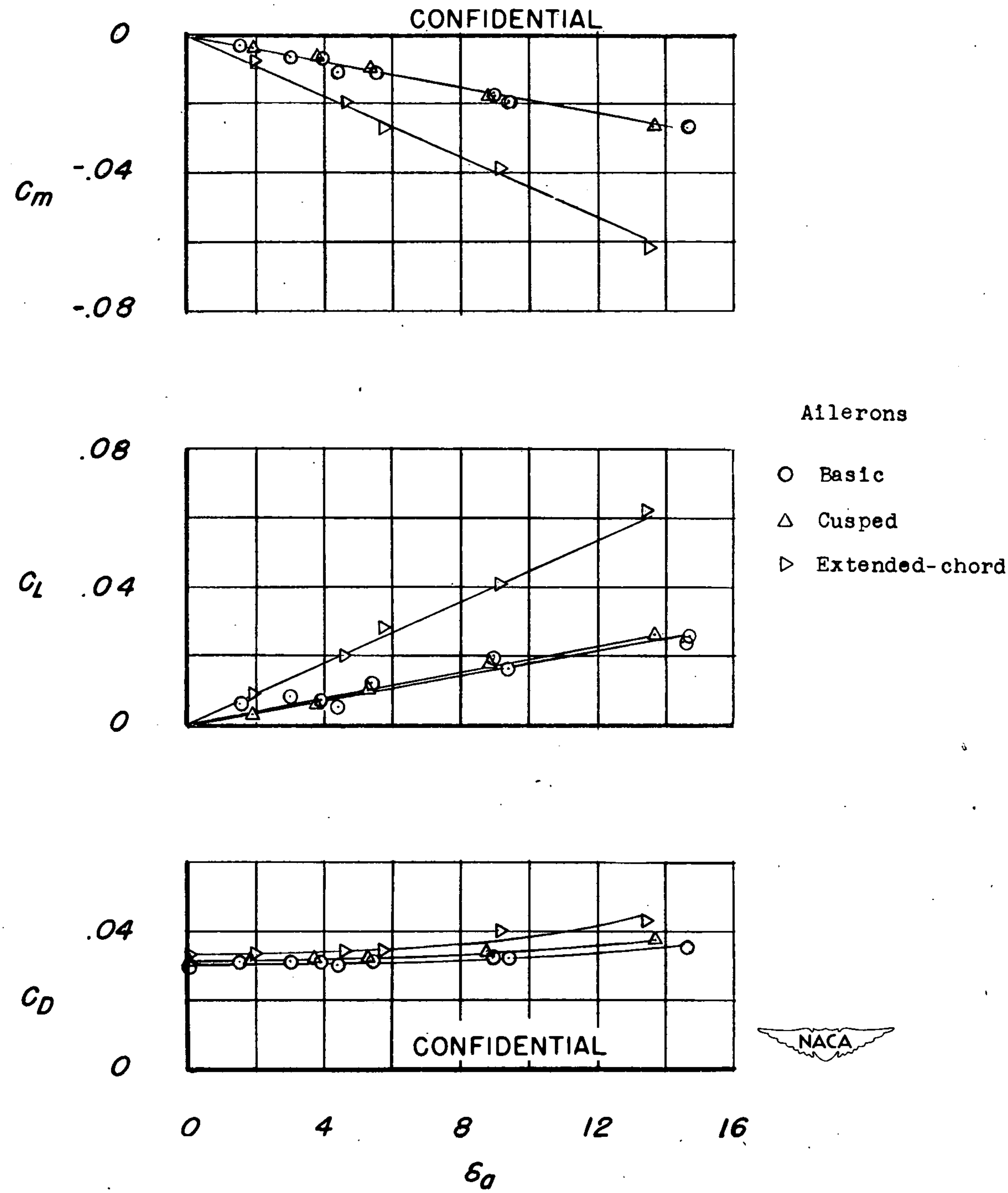

(a) Basic, cusped and extended-chord ailerons.

Figure 7.- Aerodynamic characteristics of a 42.7° sweptback wing with each of 6 types of outboard ailerons deflected. Fuselage off; $\alpha = 0^{\circ}$; M = 1.9; R = 2.2×10^{6}. Symbols designate cross-plot points taken from faired curves.

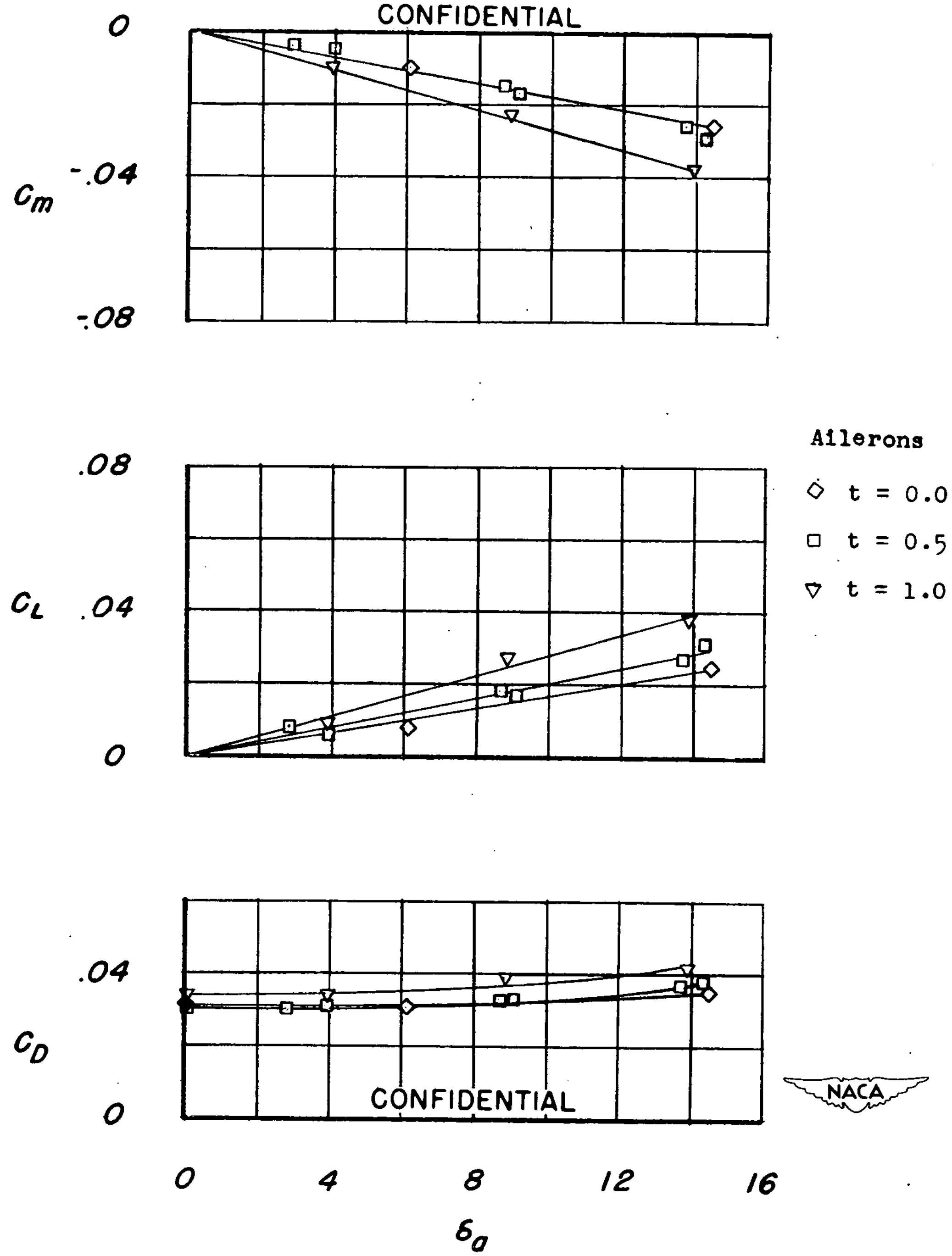

(b) t = 0.0, t = 0.5 and t = 1.0 ailerons.

Figure 7.- Concluded.

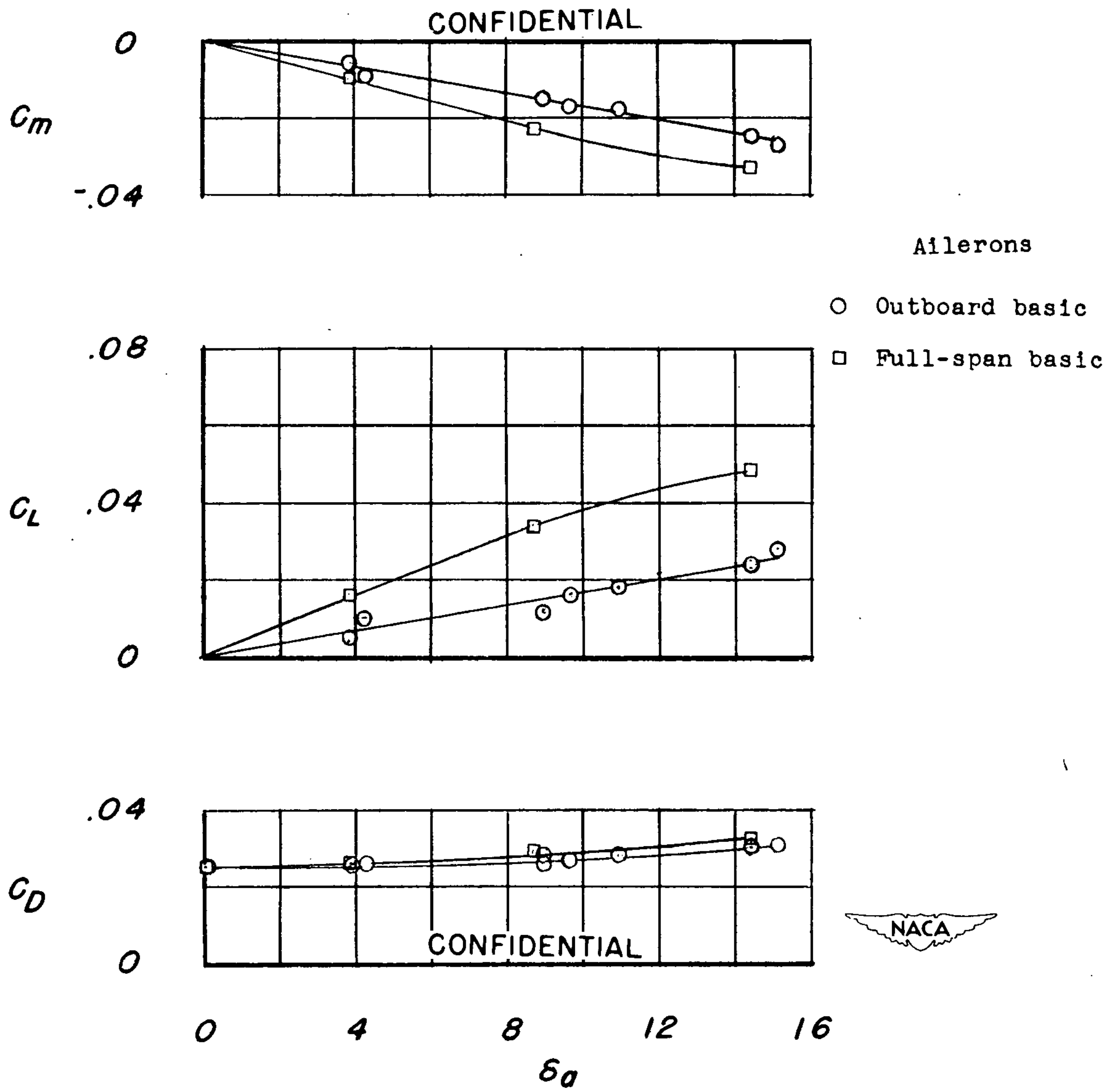

Figure 8.- Aerodynamic characteristics of a 42.7° sweptback wing with outboard basic and full-span basic ailerons deflected. Fuselage on; $\alpha = 0^\circ$; M = 1.9: R = 2.2×10^6. Symbols designate cross-plot points taken from faired curves.

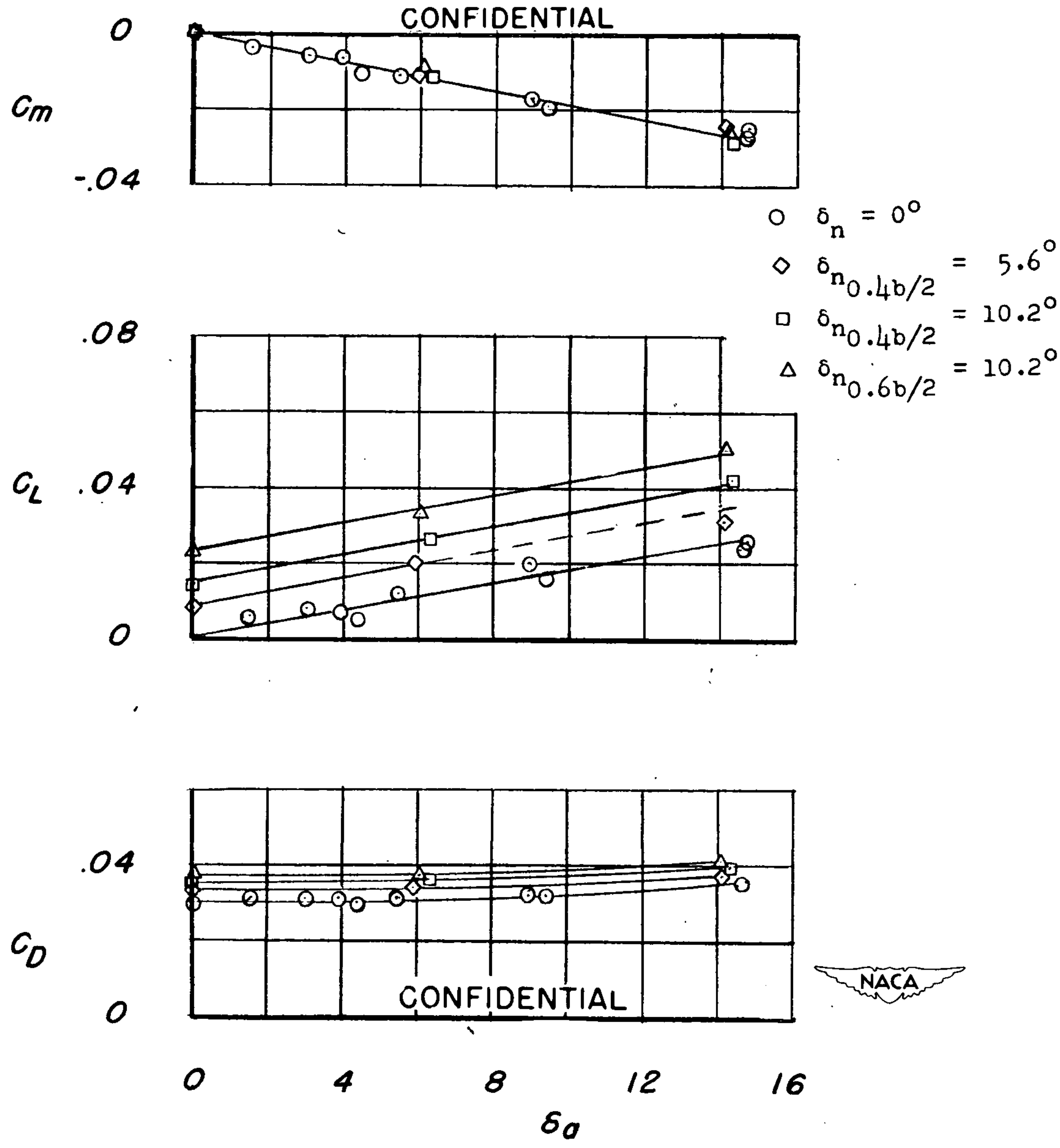

Figure 9.- Aerodynamic characteristics of a 42.7° sweptback wing with outboard basic aileron and 0.15c nose flaps deflected. Fuselage off; $\alpha = 0°$; $M = 1.9$; $R = 2.2 \times 10^6$. Symbols indicate cross-plot points taken from faired curves.

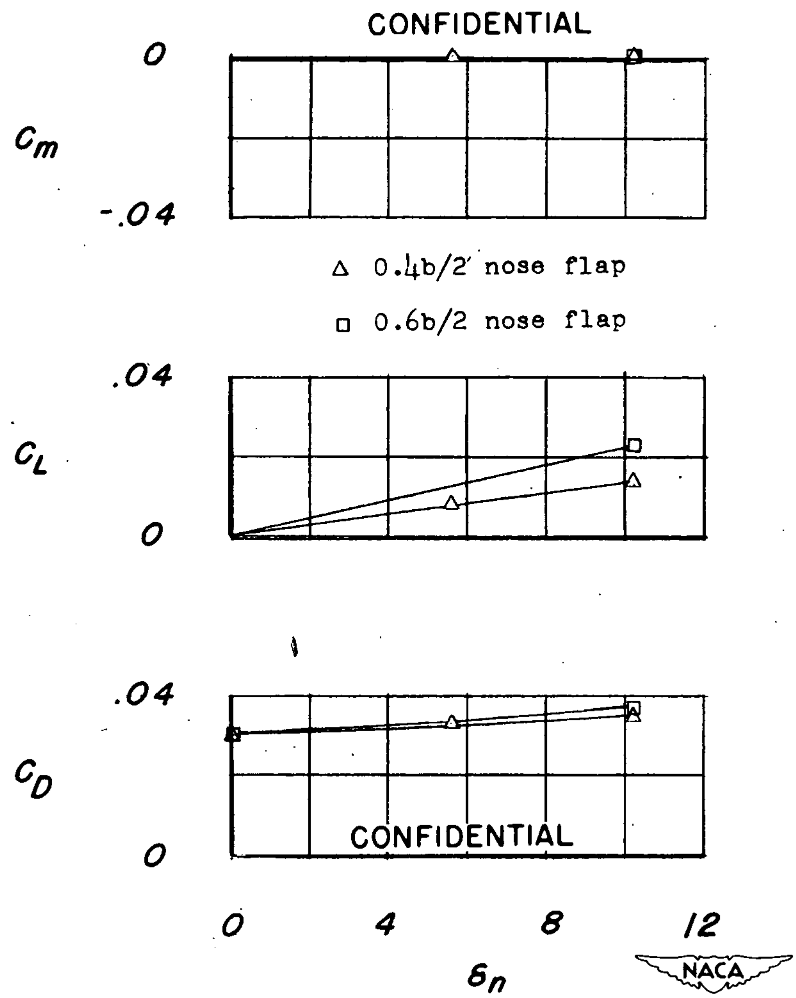

Figure 10.- Aerodynamic characteristics of a 42.7° sweptback wing with 0.15c nose flaps deflected. Fuselage off; $\alpha = 0^{\circ}$; $M = 1.9$; $R = 2.2 \times 10^6$. Symbols indicate cross-plot points taken from faired curves.